HOSTED BY

ELSEVIER

Available online at www.sciencedirect.com

ScienceDirect

Soils and Foundations 60 (2020) 342–355

SOILS AND FOUNDATIONS

www.elsevier.com/locate/sandf

Technical Paper

Development of thermal and deformation stability of Qinghai-Tibet Highway under sunny-shady slope effect in southern Tanglha region in recent decade

Yi Song [a,c], Long Jin [b,c,*], Hui Peng [b], Hongyuan Liu [c]

[a] State Key Laboratory of Loess and Quaternary Geology, Institute of Earth Environment, Chinese Academy of Sciences, Xi'an 710075, China
[b] State Key Laboratory of Road Engineering Safety and Health in High-altitude Regions, CCCC First Highway Consultants Co., LTD, Xi'an 710075, China
[c] College of Science and Engineering, University of Tasmania, Hobart 7005, Australia

Received 27 March 2017; received in revised form 16 December 2019; accepted 20 January 2020
Available online 10 April 2020

Abstract

The Qinghai-Tibet Highway (QTH) crosses 528 km of a permafrost region in the Qinghai-Tibet Plateau, half of which has suffered freezing-thawing damage induced by the sunny-shady slope effect (SSSE), especially in the Southern Tanglha Region (STR). Given this problem, a continual field investigation was carried out in the STR to examine the types of damage and the development characteristics of the affected embankments. The investigation indicated that up to 60% of the damage featured an asymmetric specialty, mainly comprising uneven thaw deformation and longitudinal cracks. Furthermore, the long-term monitoring data taken from four observation sites in a recent decade, including the shallow soil temperature, ground temperature, freezing-thawing processes, and deformation, were used to analyze the thermal-deformation process of the embankments as well. Under the SSSE, the temperature fields of the embankments were characterized by the increase in ground temperature, the descent of the permafrost table, and the expansion of the thawing period in the sunny slopes during the operation period, representing several remarkable asymmetric phenomena. Specifically, the maximum difference between the annual average shallow soil temperatures of the sunny and shady slopes reached 3.17 °C. In addition, the permafrost table on the sunny slope side was about 1.0 m lower than that on the shady slope side because the thawing period is 1–2 months longer each year on the sunny slope side. Correspondingly, the asymmetric thermal state of the embankments led to varying degrees of asymmetric deformations. The heat budget calculation showed that the route direction was the most significant factor of influence on the SSSE. The embankment height was also seen to have a remarkable influence on the SSSE.

Keywords: Qinghai-Tibet Highway; Permafrost; Embankment stability; Sunny-shady slope effect

1. Introduction

Frozen soil is made up of solid mineral particles, ice inclusions, liquid water (unfrozen water and tightly bound water), and gaseous inclusions (water vapor and air) (Tsytovich, 1985). Permafrost is a particular type of soil that is highly sensitive to changes in temperature. The main engineering problem encountered in permafrost regions is the thawing of the permafrost, which becomes even severer when the effects of global warming are taken into account and the safety of engineering operations is seriously affected (Gao et al., 2015; Wu and Zhang, 2008). For road engineering, it is vital that the geological hazards and engineering problems resulting from the thawing of permafrost

* Corresponding author at: State Key Laboratory of Road Engineering Safety and Health in High-altitude Regions, CCCC First Highway Consultants Co., LTD, Xi'an 710075, China.
E-mail address: jlcoolmail@163.com (L. Jin).

https://doi.org/10.1016/j.sandf.2020.01.012

foundations be taken into consideration (Jin et al., 2012). In China, the Qinghai-Tibet Highway (QTH) is one of the most critical passageways connecting inland China and the Qinghai-Tibet Plateau, of which 550 km is over permafrost. Since asphalt pavement was laid on the highway in 1973, 60% of the permafrost under the embankments has degenerated because of an increase in the mean annual ground temperature (MAGT). The MAGT is the ground temperature below a certain depth which does not change in a year. The decrease in the permafrost table and the increase in the thickness of the active layer are the greatest evidence of the thawing of permafrost (Peng et al., 2015a, 2015b; Wu and Zhang, 2010; Wu et al., 2015; Zhao et al., 2010). Based on survey data, the permafrost-related damage rate along the QTH was approximately 31.7% in 1990, 85% of which resulted from the thawing of the permafrost foundation (Cheng et al., 2008). To solve this problem, it was proposed that the height of the embankments be raised. This method of raising the embankment height is now widely used in practical engineering. It has been found to be able to effectively control the deformation and to increase the stability of the embankments in permafrost regions (Jin et al., 2012). However, based on the continuously monitored data, more forms of asymmetrical damage to the embankments have gradually developed since the height of the embankments along the QTH was increased in 2003. The forms of asymmetrical damage to the embankments comprise uneven thaw deformation and longitudinal cracks in the transverse section, which have become the primary types of damage on the QTH (Wang et al., 2019a).

The asymmetrical damage is mainly induced by the deviation of the thaw bowl beneath the embankments, which results from the sunny-shady slope effect (SSSE) of the embankments. In permafrost, the development of thaw-induced embankment settlement is distinctly different between the sunny and shady slopes of embankments, namely, a slope-directive difference. When the route direction follows an east-west trend, the southern slope of embankments is exposed to sunshine for more extended periods during the year. Hence, the heat absorbed by the sunny slopes is much greater than that absorbed by the shady slopes, which leads to higher ground temperatures and more in-depth permafrost tables in the sunny slopes. Correspondingly, a transverse asymmetrical temperature field is formed. Moreover, embankments with a higher elevated height lead to larger areas of the sunny and shady slopes being exposed to sunshine, which can further increase the difference in heat absorption. Therefore, the higher the embankment fill and the more the route follows the east-west trend, the greater the SSSE and the more significant the asymmetry of the thaw-induced embankment settlement. After several years of reconstruction, the embankment heights of the QTH have generally reached 3.0–4.0 m, giving rise to a gradually significant SSSE on the embankments of the QTH (Song et al., 2013; Wu et al., 2014).

The SSSE has been confirmed by more and more observations (Sheng et al., 2005; Chou et al., 2010; Liu et al., 2019). To solve the problems caused by the SSSE, some researchers have developed theoretical methods to investigate the thermal-deformation stability of highways under the SSSE (Chou et al., 2008, 2010, 2015; Tai et al., 2018). Several special measures, such as the use of thermosyphon (Song et al., 2013; Wu et al., 2014; Pei et al., 2018; Pei et al., 2019), crushed-rock (Lai et al., 2006), riprap slope protection (Lai et al., 2004), and duct-ventilated embankments (Niu et al., 2006; Yu et al., 2005), have been implemented to improve the thermal stability of embankments. However, given the great difficulty of precise heat regulation on the embankments experiencing the SSSE under the action of multiple factors, including the road route, embankment height, and permafrost geology, etc., some new embankment problems, such as waved deformation and frost cracks resulting from insufficient or excessive regulation, have gradually emerged during the operation time (Wang, et al., 2019a).

Moreover, most of the past research on the SSSE was conducted through numerical simulations, model tests, and short-term field investigations (Chou et al., 2008; Chou et al., 2010; Liu et al., 2016; Zhang et al., 2017; Wang et al., 2019b). Few studies have investigated the asymmetrical damage to embankments caused by the SSSE based on a series of long-term field investigations. To examine the thermal and deformation stability of embankments affected by the SSSE, the embankments in the southern section of the QTH are considered in this study. Firstly, the paper examines the existing thermal hazards caused by the SSSE along the QTH. Then, monitoring data from four embankment sections with different route trends and embankment heights, including monitored shallow soil temperature, ground temperature, and deformation data, collected over a period of 10 years, are used to thoroughly investigate the changing process of the asymmetrical damage to the embankments under the SSSE. The findings herein could provide technological support for the proper design and construction of highways in permafrost regions.

2. Overview of the study area

The study was carried out in the southern section of the QTH, called the Southern Tanglha Region (STR), which begins in the Tanglha Mountains and ends in Amdo (Fig. 1). Briefly, the climate characteristics of the STR include intense solar radiation, long hours of sunshine, and low air temperature. Specifically, the radiation intensity in this region is more than 8000 MJ/m^2, which is approximately five times greater than that in mainland China. The mean annual air temperature falls in the range of −5 °C to 0 °C, and the average altitude is higher than 4000 m.

The section of the QTH with the highest elevation runs through the Tanglha Mountains. Moreover, this section of the QTH has the most complicated geological conditions

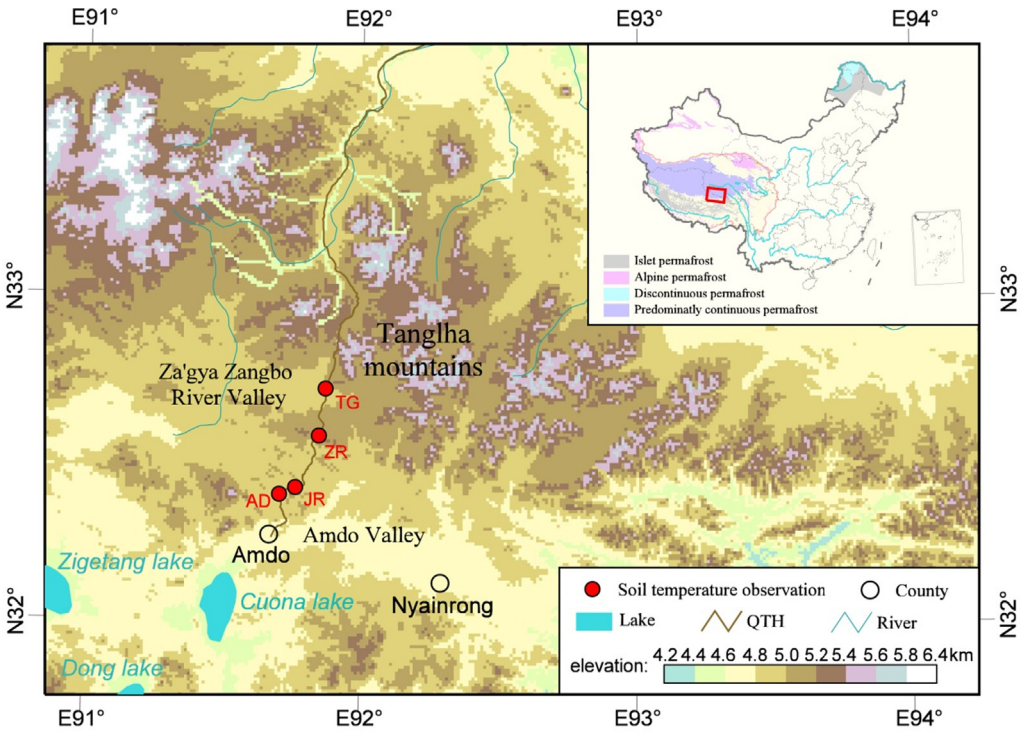

Fig. 1. Schematic location of monitoring sites TG (Tanglha Mountains), ZR (Za'gya Zangbo River), JR (Jiebuqu River), and AD (Amdo) in STR of Qinghai-Tibet Plateau (Modified after Li and Cheng, 1996; Wang, 2006).

and was correspondingly the most challenging section of the QTH to construct. The Tanglha Mountains form a watershed that separates the two river systems flowing into and out of the northern Tibet Plateau. Consequently, the natural environment, geological conditions, and permafrost environment of the STR greatly differ from those of the Northern Tanglha Regions. In the STR, wetlands are widely distributed on the southern slopes where the vegetation mainly consists of alpine steppes. Permafrost develops immensely in the STR, including mainly warm and ice-rich frozen soil.

According to the topographic features and permafrost geological environment, the engineering corridor of the QTH in the STR can be divided into three parts. Part I is the Tanglha Mountains area, in which the average altitude exceeds 5000 m. It is the source of many rivers in China, such as the Yangtze, Lancang, and Nu Rivers. This perpetually snow-covered mountain area has a hugely undulating terrain and the climate difference between the northern and southern slopes is enormous. Specifically, the climate on the northern slope is dry and lacks rainfall, which induces remarkable desertification. However, lush vegetation grows on the southern slope due to the warm and rainy climate there. The altitude is the main factor in the permafrost development in this area. Based on the monitoring data, the permafrost is mainly classified as consisting of low-temperature frozen soils (MAGT < -1.5 °C).

Part II includes the Za'gya Zangbo River Valley, which is an alluvial plain formed by a river. It is flat with an average altitude of approximately 5000 m. The climate in the valley is warm and rainy. The layers are mainly Quaternary overburden strata, which mostly consist of silty clay, silt, and fine sand. The permafrost in this area mainly consists of warm and ice-rich frozen soils with an MAGT higher than -1.5 °C.

Part III is the Amdo Valley, which mainly comprises a valley, an alluvia fan, low mountains, and hills. Based on the latest survey results, the southern boundary of the permafrost is near 32°18′58″N, 91°.43′34″E of the QTH in this area. The permafrost in this area is degenerating and mainly consists of warm frozen soils with an MAGT of higher than -1.5 °C.

The QTH covers a distance of 1076 km, of which 528 km extend over permafrost, including a 103-km-long permafrost section in the STR. To investigate the long-term stability of the embankments there, a long-term monitoring system was established from Xidatan to Amdo along the QTH in the permafrost regions, covering most of the continuous permafrost in this engineering corridor. In this system, the ground temperature, soil heat flux, and embankment deformation were continuously monitored. They are the objects of analysis in this study. To examine the influence of the SSSE on the thermal and settlement stability of the embankments in the STR, four monitoring sections in this region were selected; they are labelled TG, ZR, JR, and AD and are a shown in Fig. 1. The geographical information and embankment heights of these monitoring sections are summarized in Table 1.

Table 1
Geographical data and information on monitoring sections in STR.

Area	Longitude	Latitude	Altitude (m)	MAGT (°C)	Embankment height (m)	Road trend	Abbreviation
Tanglha Mountains	91°52′30″E	32°42′20″N	4951	−1.21	2.8	N48°E	TG
Za'gya Zangbo River	91°32′03″E	32°30′28″N	5002	−1.11	4.3	N8°E	ZR
Jiebuqu River	91°44′16″E	32°26′30″N	4900	−0.15	1.9	N14°E	JR
Amdo	91°42′27″E	32°23′01″N	4800	−0.16	0.8	N71°E	AD

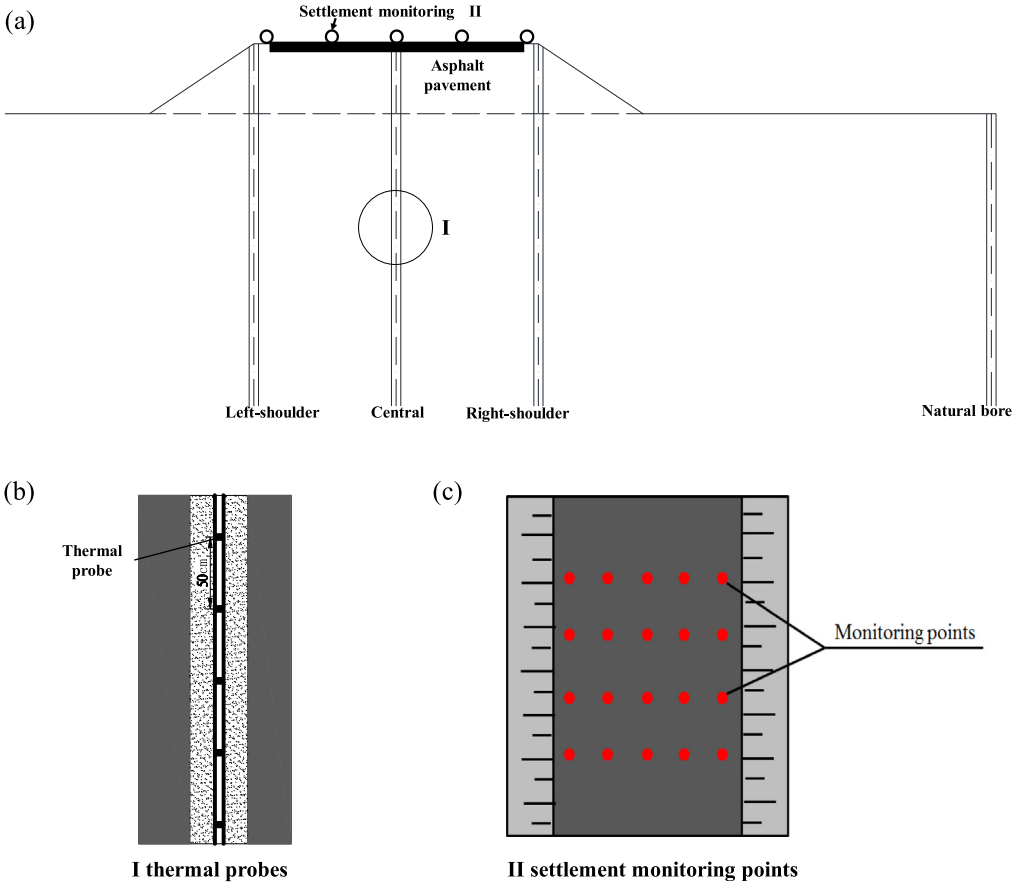

Fig. 2. Schematic diagram of monitoring section: (a) monitoring section, (b) thermal probes in temperature monitoring borehole, and (c) settlement monitoring locations.

Fig. 2 illustrates the layout of each monitoring section, which includes the ground temperature and the settlement monitoring sites. The monitoring data were collected at the beginning and middle of each month. As shown in Fig. 2(a) and (b), the ground temperature was measured using a string of thermal probes with a precision error of ±0.02 °C in each thermal probe and a spacing depth of 0.5 m along the depth. Four boreholes for temperature monitoring were drilled in each monitoring section. They include a central bore, a left-shoulder bore, a right-shoulder bore, and a natural bore, as shown in Fig. 2. As depicted in Fig. 2(c), 20 monitoring points and one reference point were designated on the embankment surface of each monitoring section. Fig. 3(a)–(d) depict the cross-sectional profile of each embankment and the original ground surface in each of the four monitoring sections, namely, TG, ZR, JR, and AD, respectively. In addition, the left and right shoulders of the embankment were determined by the direction of the route from Golmud to Lhasa.

3. Asymmetric damages to embankments in STR

The QTH was first built in the 1950s and has been reinforced several times. During the early period of its operation, the height of the embankments in many sections was elevated to prevent thawing-induced settlement, which was proven to be an efficient measure. However, several areas of asymmetric damage have emerged in these sections in recent years.

The data collected from the survey indicate that the asymmetric damage had already become the main type of damage observed in this region, accounting for up to 60% of all damage. Among the types of damage, longitudinal cracks and slope cracks constituted 58.9% of the asym-

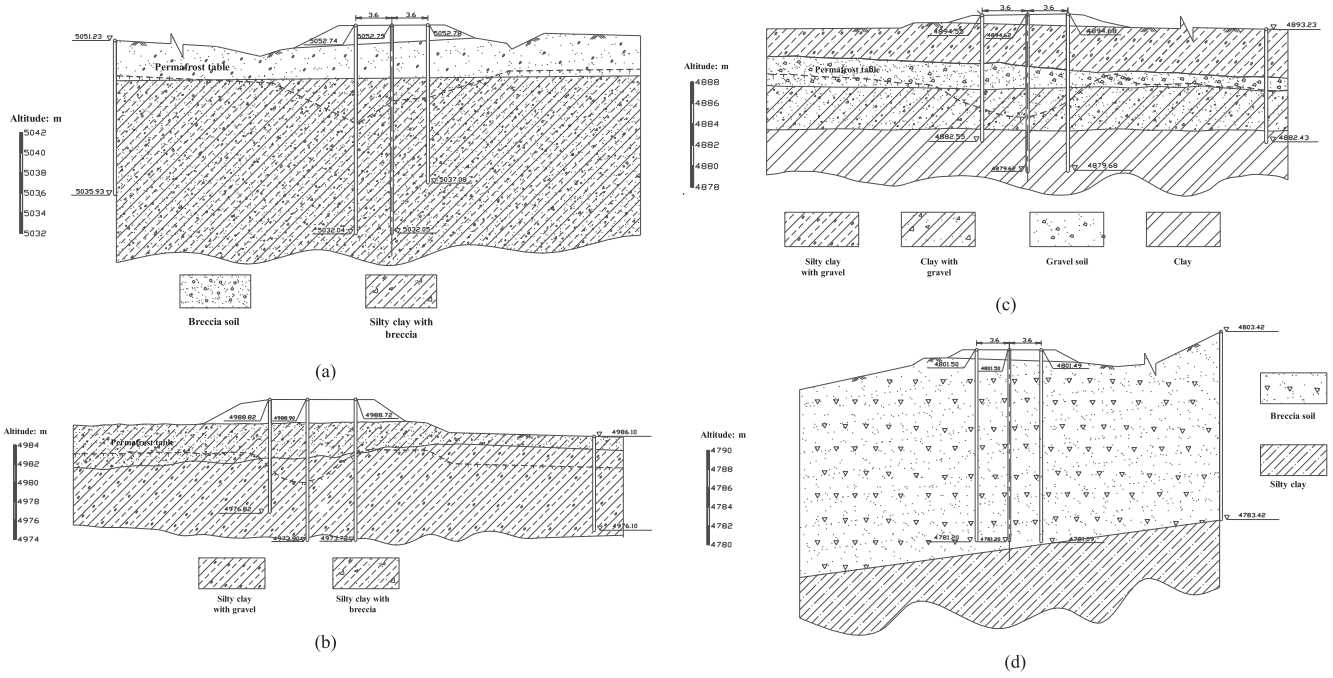

Fig. 3. Cross-sectional profile of embankment and original ground surface: (a) Tanglha Mountains (TG), (b) Za'gya Zangbo River (ZR), (c) Jiebuqu River (JR), and (d) Amdo (AD).

metric damage, as shown in Fig. 4(a). In the most devastated sections, the length of the damaged embankment exceeded 40 km, with a maximum crack width of about 40 cm. Moreover, slope collapses (Fig. 4(b)) and embankment leaning (Fig. 4(c)) were common types of damage as well.

The distribution of asymmetric damage has a marked slope-directive regularity. The survey data reveal that the asymmetric damage developing in the sunny slope accounted for 66.5% of all damage surveyed and was closely related to the embankment height. In the embankment sections with low heights (<0.5 m), asymmetric damage barely developed. However, with a rise in the embankment height, the rate of damage is seen to have gradually increased. It is noted that the asymmetric damage observed in the embankment sections with heights >3.0 m accounted for 75.7% of all surveyed damage.

4. Monitoring data and analyses

4.1. Shallow soil temperature

To investigate the differences in the shallow soil temperatures between the sunny and shady embankment slopes, the temperatures of soils at the shallow depth of 0.5 m were collected at different monitoring sections, which are shown in Figs. 1 and 3 and illustrated in Fig. 5. Moreover, the mean average shallow soil temperatures (MASSTs) are given in Table 2. It can be found from Fig. 5 that the shallow soil temperatures on the sunny slopes are higher than those on the shady slopes, but under different circumstances, as will be explained in the follow paragraphs.

At the Tanglha Mountains site, the direction of the QTH is about 48° north by east, and the embankment height is approximately 2.8 m. According to Fig. 5(a) and Table 2, the shallow soil temperatures of both the right (sunny) and left (shady) slopes are greater than those of the natural surfaces. And the difference in the MASSTs in the two shoulders reaches 1.89 °C, inferring a relatively obvious variation in the thermal boundary, which may trigger a massive difference in the heat disturbance in the underlying permafrost.

At the Za'gya Zangbo River site, the direction of the QTH is 8° north by east, which is similar to a south-north trend. However, the embankment height at this site is 4.3 m, which is 1.5 m higher than that at the Tanglha Mountains site. Fig. 5(b) shows that the shallow soil temperatures of the right (sunny) slope are higher. In addition, the difference in the MASSTs between the right and left slopes is approximately 3.17 °C, greater than that at the Tanglha Mountains site. Thus, although the route follows a nearly south-north trend, the above analysis indicates a more significant difference in MASSTs, which may be attributed to the higher embankment height.

The Jiebuqu River and Amdo sites lie in the Amdo Valley. The directions of the QTH at the two sites are 14° and 71° north by east, respectively, and the heights of the embankments there are relatively lower than at the other sites. As shown in Table 2, the differences in the MASSTs between the right (sunny) and left (shady) shoulders at the Jebuqu River and Amdo sites are 0.11 °C and 0.15 °C, respectively. Based on the results of the statistical analysis of the monitoring data, it is concluded that the MASSTs are not obvious at the two locations. The explanations

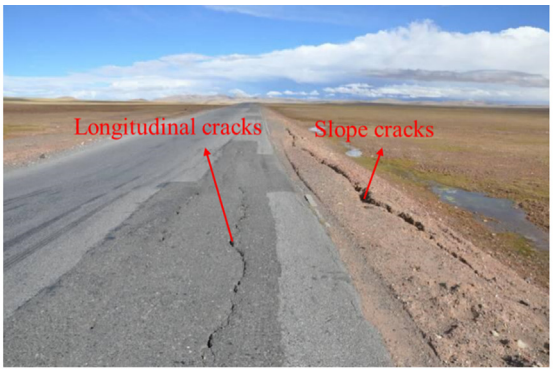

(a)

(b)

(c)

Fig. 4. Asymmetric damage along QTH: (a) longitudinal cracks and slope cracks occurring in embankment with height of 4.5 m, (b) slope collapses occurring in embankment with height of 7.5 m, and (c) leaning of embankment with height of 3.5 m.

for this are different for the two sites. At the Jiebuqu River site, the route is slightly different from that at the Za'gya Zangbo River site, which shows a big difference between the MASSTs on the left (shady) and right (sunny) shoulders, as introduced in the previous paragraph. Thus, the small difference between the MASSTs on the left (shady) and right (sunny) shoulders at the Jiebuqu River site is mainly attributed to the lower embankment height, which further validates that the difference in MASSTs primarily occurs at embankments with higher heights. However, at the Amdo site, the explanation is rather complicated. On the one hand, the route of the QTH at the Amdo site is mainly east-west, which is more conducive to inducing a difference between the two slopes. On the other hand, the relatively low embankment height may weaken this effect. Thus, the two aspects compete with one other to affect the embankment simultaneously, while the embankment height becomes the dominant factor of influence, which finally controls the changes in the shallow soil temperatures.

Based on the above analysis, the Za'gya Zangbo River site presents the most obvious difference between the MASSTs on the left (shady) and right (sunny) shoulders, which may trigger a significant SSSE and asymmetric temperature fields in the embankments there. Furthermore, it is demonstrated that the embankment height is the predominant factor of influence controlling this phenomenon.

4.2. Ground temperature

The ground temperature at different positions in the transverse section is an important index for evaluating the thermal symmetrical characteristic of an embankment. Fig. 6 shows the variations in the ground temperatures monitored at various depths of the left (shady) and right (sunny) shoulder boreholes as well as the middle borehole of the embankments in October 2014. In general, the ground temperatures in the sunny slopes are higher than those in the shady slopes, but they follow different trends in different embankment sections. Similar to the information given in Section 4.1, a more elevated embankment presents a more obvious difference in ground temperature between the two shoulders, indicating a more obvious SSSE, while a less elevated embankment presents a relatively small difference in ground temperature between the two shoulders, even though the road directions are close to east-west. This will be further explained in the following paragraphs.

As shown in Fig. 6(a), at the Tanglha Mountains site, the ground temperature vs depth curves demonstrate that the ground temperatures in the left shoulder (shady side) at depths of less than −10.0 m are much lower than those in the right shoulder (sunny side). The maximum difference in temperature between the two shoulders is approximately 1.6 °C at a depth of −7.6 m. Considering the shapes of the ground temperature vs depth curves, the primary differences in temperature between the two shoulders occurred at depths from 0.0 m to −10.0 m.

As shown in Fig. 6(b), at the Za'gya Zangbo River site, the ground temperature vs depth curves are different from those at the Tanglha Mountains site. The differences in ground temperature between the two shoulders at shallow depths are much more visible; they can reach a maximum value of 1.8 °C at a depth of −2.5 m, higher than that of the Tanglho Mountains site. Then, with an increase in depth, the difference gradually decreases and reaches 0.4 °C at a depth of −5.0 m.

At the Jiebuqu River and Amdo sites, the shapes of the ground temperature vs depth curves are similar to those

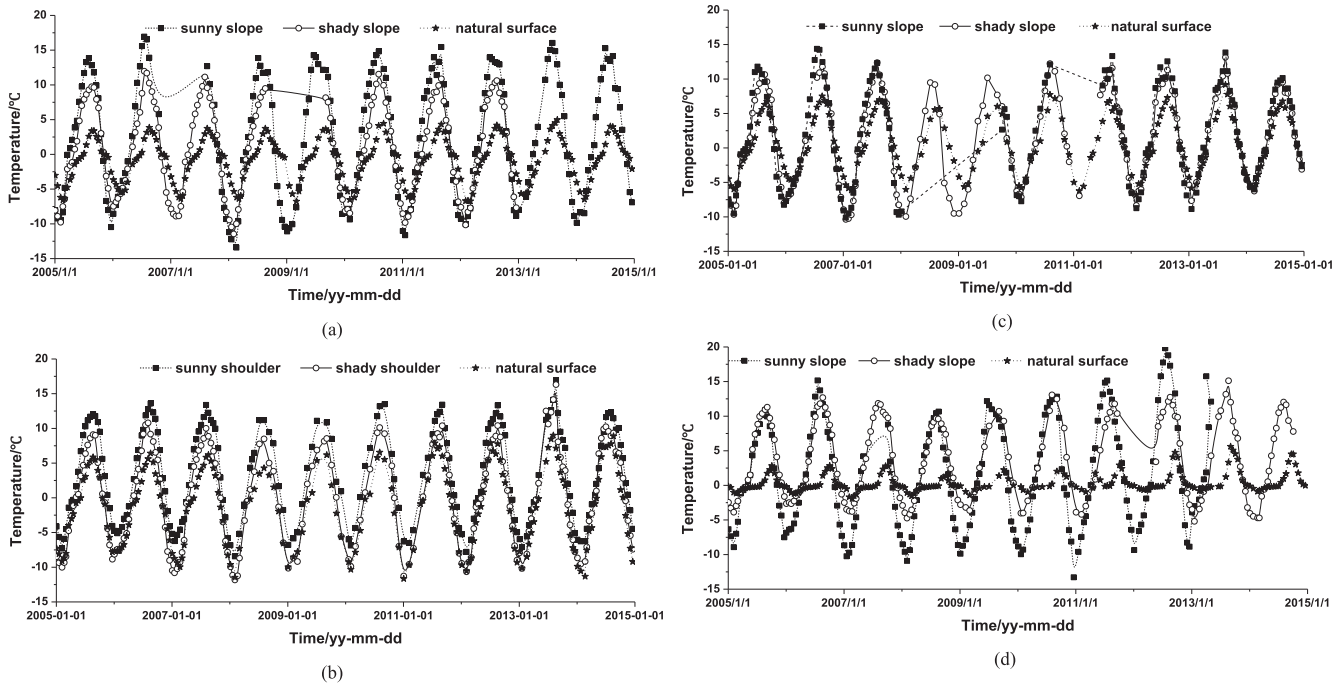

Fig. 5. Changes in shallow soil temperature in recent decade: (a) Tanglha Mountains (TG), (b) Za'gya Zangbo River (ZR), (c) Jiebuqu River (JR), and (d) Amdo (AD).

Table 2
MASSTs on right and left shoulders and natural surface (°C).

Area	Right shoulder	Left shoulder	Natural surface
TG	2.65	0.76	−0.89
ZR	3.36	0.19	−1.22
JR	2.88	2.77	0.93
AD	3.62	3.77	0.91

obtained for the Za'gya Zangbo River site, as illustrated in Fig. 6(c) and (d), respectively. However, since the Jiebuqu River and Amdo monitoring sites are close to the south boundaries of permafrost, the permafrost at depths of less than −10.0 m on both the sunny and shady sides is in a seriously degraded status, and some of it has degenerated (Fig. 6(d)).

4.3. Depth of the permafrost table

The thermal difference between the sunny and shady slopes will cause the difference between the permafrost tables under the two slopes. It can then be inferred there is an active layer with inhomogeneous thickness in the transverse section of the embankments, which will result in the uneven settlements of the embankments, and then induce asymmetrical damage. Hence, the permafrost table is also a valid index that reflects the asymmetric characteristics of the embankments. Thus, the permafrost table was analyzed to investigate the SSSE of the embankments. Fig. 7 shows the variations in the permafrost tables under the left (shady) and right (sunny) shoulders of the embankments monitored between 2005 and 2015.

It can be seen from this figure that the permafrost table at each monitored section is continuously increasing. In relatively cold permafrost regions, including the Tanglha Mountains and Za'gya Zangbo River sites (MAGT < −1.0 °C), the maximum depth of the permafrost table reaches 8.65 m and 7.60 m under the sunny and shady shoulders, respectively. At the Tanglha Mountains site, the permafrost table under the sunny shoulder is decreasing at an average rate of 0.20 m/year, which is 2.22 times faster than that under the shady side. At the Za'gya Zangbo River site, the average decreasing rate of the permafrost table under the sunny shoulder is the same as that at the Tanglha Mountains site. However, under the shady shoulder, the average rate is 1.25 times faster than that observed at the Tanglha Mountains site.

In warm permafrost regions (Jiebuqu River site and Amdo site with MAGT > −0.5 °C), the rate of the decrease in the permafrost table is relatively more significant, particularly at the Amdo site, where the depth of the permafrost table decreased from 9.95 m (in 2005) to 13.14 m (in 2014) under the right (sunny) shoulder. The average decreasing rate reaches 0.312 m/year, 1.5 times faster than that observed in cold permafrost regions. However, at the Jiebuqu River site, the degeneration of the permafrost table exhibits a different phenomenon. As shown in Fig. 7(c), although the depth of the permafrost table is higher under the left shoulder (shady side), it is decreasing at a rate of 1.54 times greater than that under the right shoulder (sunny side). Following this trend, the permafrost tables

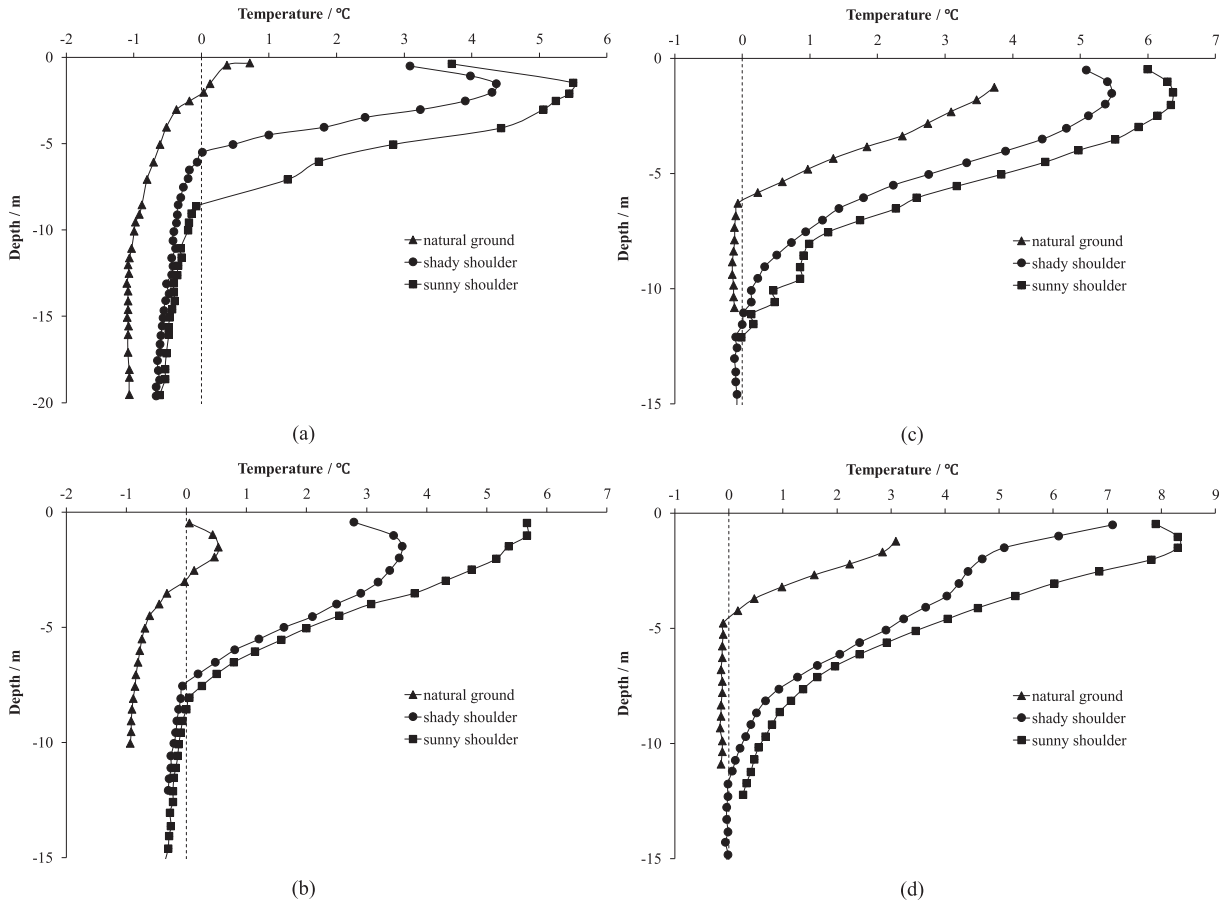

Fig. 6. Deep geothermal curves (2014.10.18): (a) Tanglha Mountains (TG), (b) Za'gya Zangbo River (ZR), (c) Jiebuqu River (JR), and (d) Amdo (AD).

under both slopes would tend to be the same. Therefore, it is predicted that the embankment ground temperature field will gradually become symmetrical in the future, which is mainly attributed to an approximate south-north route direction and a weakened SSSE resulting from the lower embankment height.

4.4. Freezing-thawing process

To further investigate the evolution of the asymmetrical damage with the passage of time, Fig. 8 gives the evolution curves of the freezing-thawing process occurring in the sunny and shady shoulder boreholes over a 10-year period, which can reflect the significant levels of SSSE to a certain degree. Due to the malfunction of the monitoring instrument at the Tanglha Mountains site, the deep ground temperatures were insufficient over the last several years. Thus, the freezing-thawing process at this site is not given.

Overall, the thawing time of the embankment has gradually increased during the operation period. The thawing time of the sunny slope is one or two months more than that in the shady slope according to monitoring results. More, specifically, at the Za'gya Zangbo River site (Fig. 8(a)), the thawing period of the right shoulder lasted from late April to late October 2005, while the thawing period lasted from late April to late November in 2015, which is nearly 1 month longer. The other sites show similar trends. In addition, the monitoring results show that the depths of the permafrost table have continuously increased over the 10 years, with the increased depths of 3.0 m and about 1.0 m under the sunny and shady shoulders, respectively. However, a different phenomenon is observed at the Jiebuqu River site. Except for a few years, the difference between the thawing times of the two shoulders has remained about 0.3 months during this period, indicating a relatively weakened SSSE.

4.5. Embankment deformation

In permafrost regions, the embankment deformation is closely related to the permafrost degradation. Many factors affect the embankment deformation, but the thawing of the permafrost foundation is the dominant factor. Considering the SSSE, the asymmetric deformation of the embankment is the immediate cause of the asymmetric damage to the embankment in the permafrost regions. Fig. 9 shows the varying embankment deformation processes occurring at all the monitoring sites in the STR from

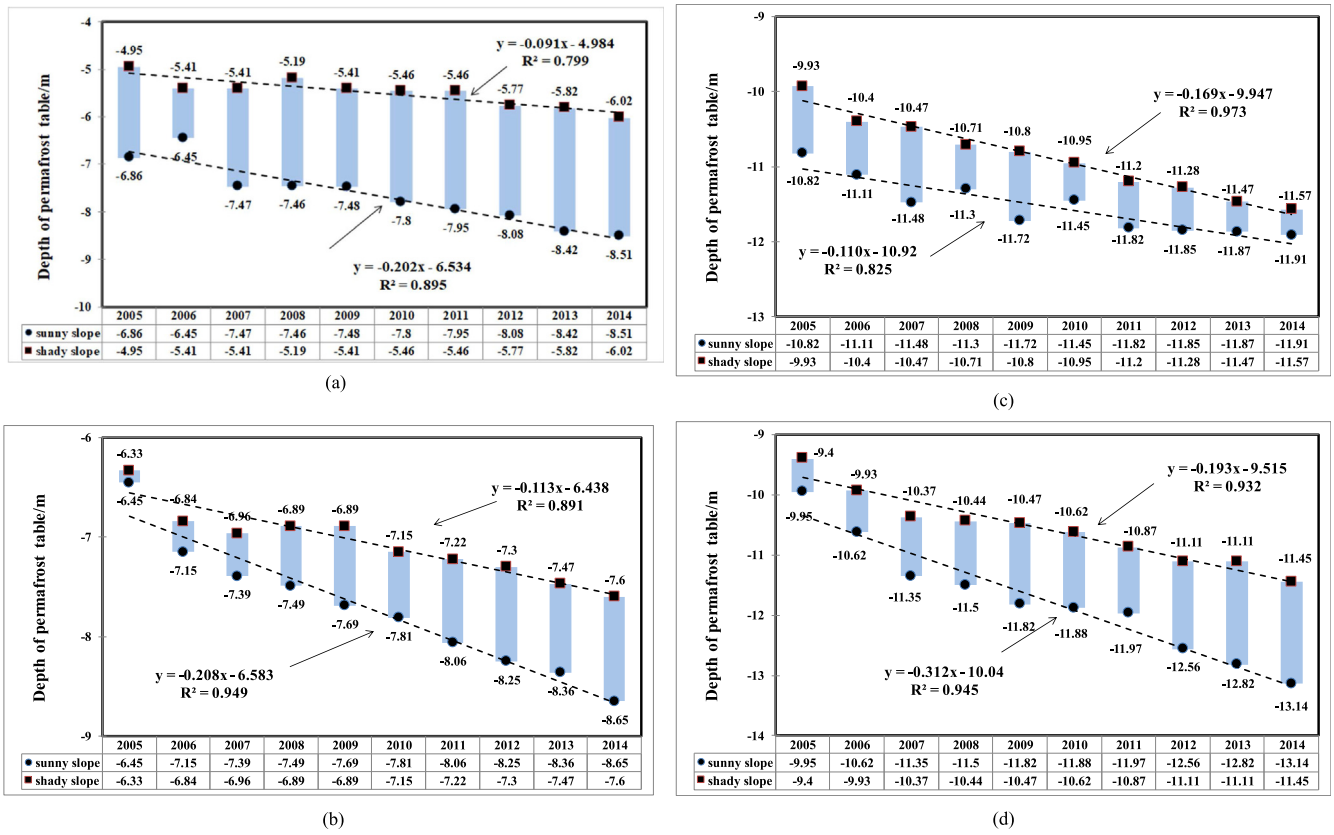

Fig. 7. Changes in permafrost table in recent decade: (a) Tanglha Mountains (TG), (b) Za'gya Zangbo River (ZR), (c) Jiebuqu River (JR), and (d) Amdo (AD).

2005 to 2015. They are analyzed in the following paragraphs in terms of the time and space regularities of the asymmetric deformation.

From the time perspective, the embankments at all monitoring sites have experienced significant settlements before the monitoring and during the decade of monitoring. As can be seen from Fig. 9, the settlements of most of the embankments amount to approximately 30 cm during the recent ten-year period. The most considerable amount of settlement is observed at the Amdo site, with a maximum settlement of nearly 40 cm (Fig. 9(d)). Then, from the spatial perspective, the deformations between the sunny and shady sides are not identical in each cross section, substantiating an asymmetric characteristic of the embankment deformation. Therefore, the difference in the deformations between the two shoulders was selected to reflect the asymmetry of the embankment deformation. Fig. 9 indicates that the embankment at the Za'gya Zangbo River site has the maximum deformation difference, which is about 17.4 cm at the end of the monitoring period (Table 3). The deformation difference between the two shoulders at the Amdo site takes second place, with a difference of approximately 14.6 cm. The embankments at the Jiebuqu River site and the Tanglha Mountains site present the minimum deformation differences, namely, 1.5 and 5.1 cm, respectively. Further analysis reveals that the deformation rate on the sunny side is more considerable than that on the shady side. At the Za'gya Zangbo River site, the deformation rate on the sunny side (2.5 cm/year) is about 3.3 times larger than that on the shady side (0.8 cm/year). Hence, if there were no measures adopted to cope with the deformation difference, the deformation asymmetry in the cross section would gradually develop with the passage of time, and then induce longitudinal cracks, embankment slope collapses, and other asymmetric damages.

Based on the analysis results of the thermal condition and the deformation process of the embankments in this region, it is inferred that the varying degrees of the SSSE are the main reason for the asymmetric damage to the embankments. Accurately, at the Za'gya Zangbo River site with the relatively higher embankment, a great degree of SSSE is presented, which then leads to the most significant asymmetric deformation. At the Amdo site, with a route direction that is close to east-west, although the embankment height is only 0.8 m, the embankment shows relatively visible asymmetric deformation as well. Therefore, the highest MAGT in the STR amplifies the SSSE to a certain degree. In comparison, the embankment at the Tanglha Mountains site has the lowest MAGT and then shows a relatively slighter asymmetric deformation due to the weak effect of the SSSE. At the Jiebuqu River site, where the embankment has lower heights and a route

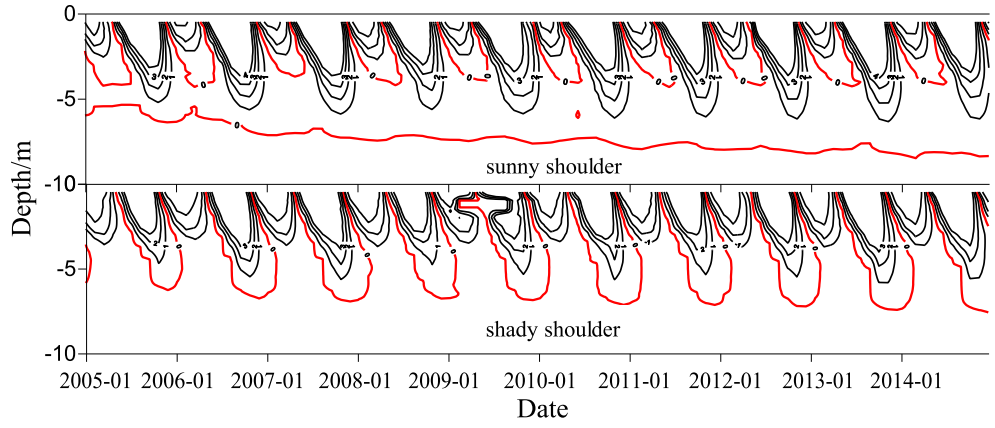

(a)

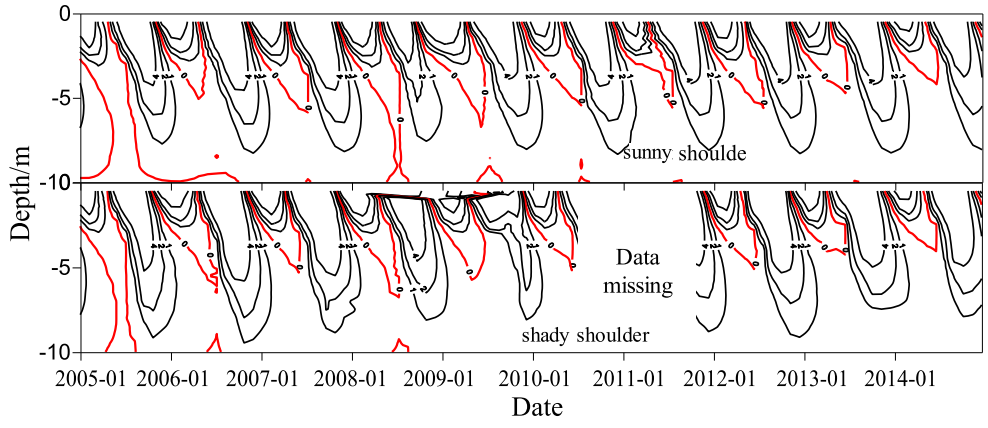

(b)

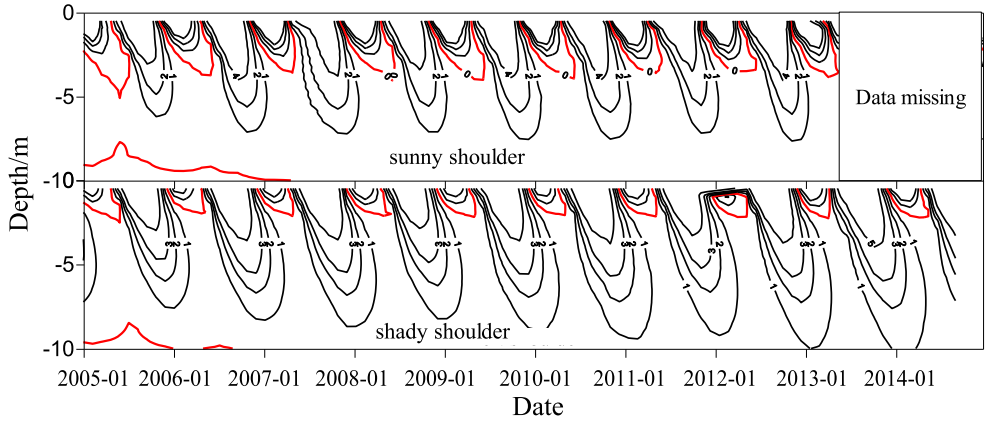

(c)

Fig. 8. Freezing-thawing process curves in recent decade: (a) Za'gya Zangbo River (ZR), (b) Jiebuqu River (JR), and (c) Amdo (AD).

direction close to north-south, the embankment expresses a slightly asymmetric deformation as well.

Therefore, it is concluded that the SSSE is governed mainly by the embankment height and the route direction. In addition, the MAGT could further influence this effect by strengthening or weakening the development of the asymmetric deformation of the embankment.

5. Discussions

5.1. Heat budget difference between sunny and shady slopes

To further quantify the SSSE, the shallow soil temperatures on the sunny and shady sides were used to evaluate the energy transfer process under the SSSE. The

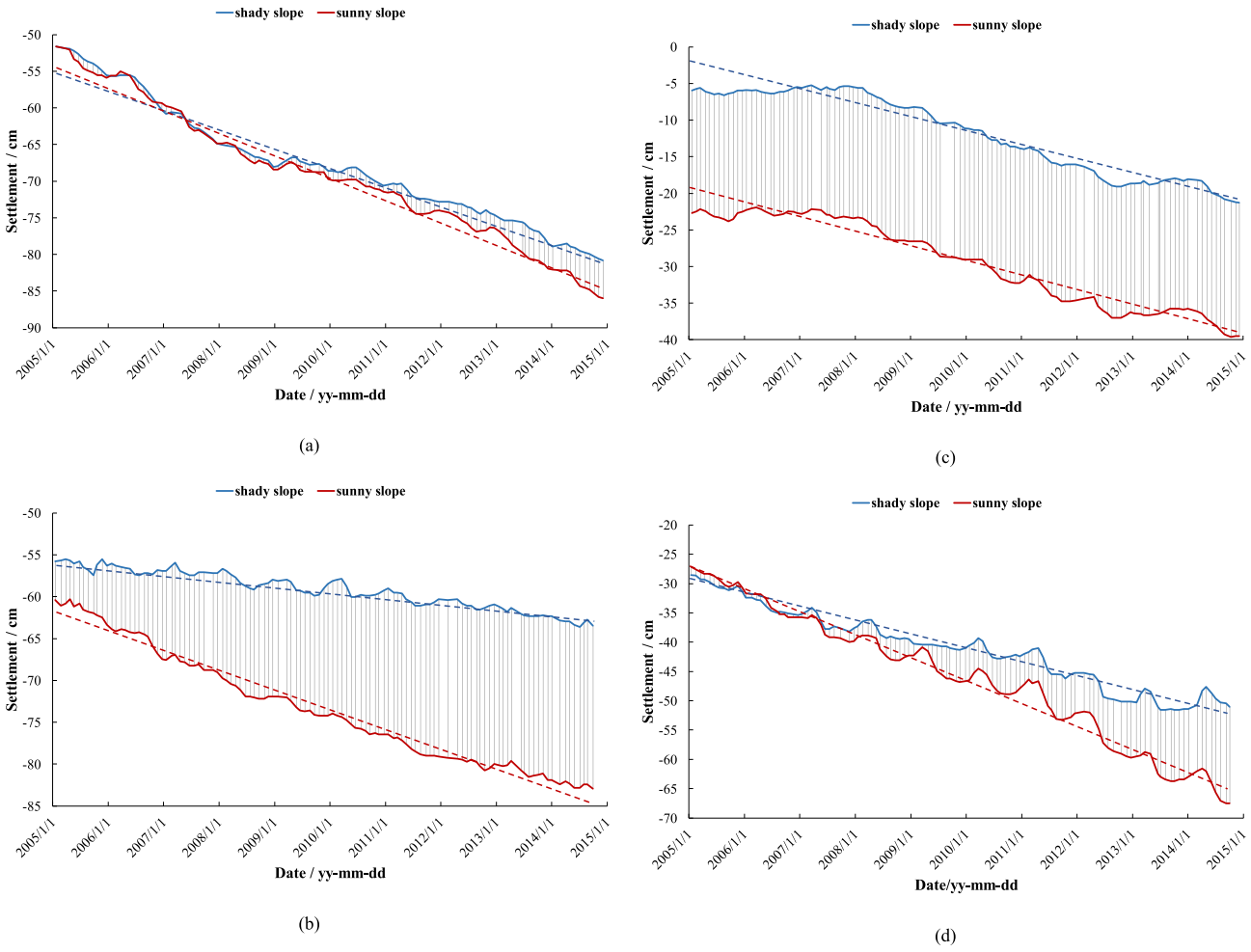

Fig. 9. Embankment deformation process in recent decade: (a) Tanglha Mountains (TG), (b) Za'gya Zangbo River (ZR), (c) Jiebuqu River (JR), and (d) Amdo (AD).

Table 3
Embankment deformation difference (cm).

Area	Deformation (cm)		Deformation difference (cm)
	Right shoulder	Left shoulder	
TG	32.9	27.8	5.1
ZR	25.2	7.8	17.4
JR	17.6	16.1	1.5
AD	39.4	24.8	14.6

calculation process involves several steps. Firstly, the vertical temperature gradient was obtained using the monitoring data. The vertical heat flux was then computed with the thermal physical parameters of the embankment filling materials. After that, the heat budget near the surface of the embankment was determined by integrating the flux in time.

Based on Fourier law, the heat flux under the surface of the embankment could be obtained using Eq. (1):

$$q = -\lambda \frac{\partial T}{\partial z} \approx -\lambda \frac{T_{h2} - T_{h1}}{h_2 - h_1} \tag{1}$$

where q is the heat flux, λ is the thermal conductivity coefficient, T is the temperature, and h_1 and h_2 are the depths.

The energy was then computed by integrating Eq. (1) with the time:

$$Q = \int q dt \approx \int \left(-\lambda \frac{T_{h2} - T_{h1}}{h_2 - h_1} \right) dt \tag{2}$$

where Q is the energy transferred near the embankment surface.

Table 4 summarizes the thermal budget of the sunny and shady slopes calculated with the above procedure for the Za'gya Zangbo River site from 2005 to 2014. As can be seen, the energy transmission process reveals that the shady side continuously maintains a heat release condition, indicating a trend consistent with that of the natural borehole. On the contrary, the sunny side presents a distinct heat absorption process in the same period.

Moreover, considering the local permafrost difference, an energy-normalized index was proposed in Eq. (3) to evaluate the significance of the SSSE quantitatively.

$$\varphi = \left| \frac{Q_{sunny} - Q_n}{Q_n} - \frac{Q_{shady} - Q_n}{Q_n} \right| \quad (3)$$

where φ is the normalized index, and Q_{sunny}, Q_{shady}, and Q_n are the energies transferred into the sunny side, shady side, and natural borehole, respectively.

Based on Eqs. (1)–(3), the annual mean φ at the Za'gya Zangbo River site was calculated as shown in Table 4. Moreover, Table 5 gives the thermal budget of the sunny side, shady side, and natural borehole and the average values of φ calculated for different sites from 2005 to 2015.

5.2. Influence factors of SSSE

As can be seen from Table 5, the Amdo site presents the most remarkable SSSE, almost twice the effect of that at the Za'gya Zangbo River site, featuring an approximate east-west route and the lowest embankment height. Hence, the route direction could very likely be one of the most influential factors causing the SSSE. The Za'gya Zangbo River site expresses a secondary significance of the SSSE. In contrary to the Amdo site, the Za'gya Zangbo River site has an approximate north-south route and the highest embankment height. Thus, the embankment height is an important influential factor, too. However, although the Tanglha Mountains site has a relatively visible embankment height and a more similar east-west route than the Za'gya Zangbo River site, it exhibits the most unremarkable SSSE only because of the lowest MAGT at this site. For the Jiebuqu River site, due to its moderate height and unobvious east-west route, it shows a relatively unremarkable SSSE as well.

Therefore, the route direction was found to be the most significant factor of influence in controlling the SSSE and the embankment height had a considerable effect on the SSSE, too. Thirdly, the MAGT expresses a strengthening or weakening influence on the SSSE to a certain degree.

5.3. Influence from engineering properties of soil

Settlement occurs mainly because of the thawing of the permafrost under an embankment. For frozen soil embankments, the asphalt pavement disturbs the natural hydrothermal balance, thus inducing permafrost degeneration to a certain degree. Due to the significant mechanical differences in the soils between the freezing and thawing conditions, a thawing bowl forms under an embankment, and thus, contributes to the remarkable thawing-induced settlement, which is the considerable component of the embankment deformation in permafrost regions. Recent studies have shown that the deformation process of embankments is mainly influenced by the size and location of the thawing bowl (Wang et al., 2015; Yu et al., 2016; Zhang et al., 2017; Ming et al., 2018). Thus, for the parts of the embankments featuring similar east-west routes and relatively high heights, it should be noticed that the difference in the heat transfer conditions between the sunny and shady slopes cause a remarkable difference in ground temperature, which will then result in varying degrees of thawing bowl deviation (Zhang et al., 2019). For the above reasons, several cases of asymmetric embankment damage develop, such as uneven deformation, longitudinal cracks, and slope collapses. In addition, freezing-thawing cycles and a variation in the water (ice) content also contribute to the deformation and strength of frozen soil embankments (Jia et al., 2019; Shen et al., 2020), which should be given more attention.

When permafrost thaws under the effect of gravity, combined with the external load, the soil will proceed to thaw and consolidate, leading to large deformation. Thus, the engineering properties of the soils under embankments, especially the thaw settlement property, are important factors of influence for embankment stability. Hence, it is the thaw settlement coefficient that is an essential parameter in frozen soil engineering. It embodies the thaw deformation characteristic of permafrost and can be obtained using Eq. (4).

Table 4
Annual mean φ at Za'gya Zangbo River site.

Year	Heat from surface (J/m^2)			φ
	Shady slope	Sunny slope	Natural hole	
2005	−28402	22,044	856	58.9
2006	−7115	16,587	8367	2.8
2007	−1441	23,686	−3326	10.6
2008	−27850	13,217	−11534	3.6
2009	Data missing	38,833	−19938	–
2010	−9497	42,193	5312	9.7
2011	−21575	10,256	−9344	3.4
2012	−36007	20,047	−5251	10.7
2013	−1171	22,453	9758	2.4
2014	−30323	25,098	−4983	11.1
Average	−16872	23,597	−3437	6.8

Table 5
Average values of φ at different sites.

Area	Heat from surface (J/m^2)			φ	Influence factors
	Shady slope	Sunny slope	Natural hole		
TG	−10065	−9587	−12180	0.3	MAGT
ZR	−16872	23,597	−3437	6.8	Embankment height
JR	−17405	−16710	−3326	0.6	Route direction, Embankment height
AD	−19323	15,258	−3110	11.8	Route direction, MAGT

Table 6
Thaw settlement coefficients.

Area	Ice content (%)	Soil type	Thaw settlement coefficient	Bulk density* (g/cm^3)	Grain density* (g/cm^3)
TG	30–33	Breccia soil, silty clay with breccia	16	2.02	2.70
ZR	18–25	Silty clay with gravel	10	1.97	2.68
JR	13–17	Silty clay with gravel	5	2.04	2.73
AD	27–29	Breccia soil, silty clay	12	2.08	2.71

* Sampling depths: TG: 4.5 m, ZR: 5.3 m, JR: 3.3 m, and AD: 4.3 m.

$$a_0 = \frac{\Delta h_0}{h_0} \tag{4}$$

where a_0 represents the thaw settlement coefficient, h_0 is the thaw deformation of the testing sample, and h_0 is the initial height of the sample.

To further analyze the influence of the engineering properties of soils on the embankment settlement process, the thaw settlement coefficients of the soils at the four monitoring sites were calculated; they are summarized in Table 6. Moreover, the water content (ice content), bulk density, and grain density of the soils at all the sites are given in Table 6 as well. At the field site, typical soil samples were collected by drilling. Then, the sealed samples were sent to the laboratory for analysis. The thaw settlement coefficient was obtained by conducting thawing compression tests, and the ice content and density were obtained through the oven drying method in the laboratory following the standard for the geotechnical testing method in China (Ministry of Water Resources of China, 2019).

The Tanglha Mountains site has the maximum ice content and the maximum thaw settlement coefficient; however, it shows an unobvious SSSE due to the minimum deformation difference, although it presents relatively high overall settlements. Both the Za'gya Zangbo River site and the Amdo site have relatively high thaw settlement coefficients and present significant uneven deformation and considerable settlement between both slope sides combined with the great SSSE. The Jiebuqu River site has the minimum thaw settlement coefficient and shows the most unremarkable deformation difference. Generally, the thermal boundary difference from the SSSE makes up the external environment for the asymmetric damage to the frozen soil embankment, while the engineering properties of the soil is the crucial internal factor controlling the embankment settlement.

6. Conclusion

The Qinghai-Tibet Highway (QTH) was constructed across a permafrost region and has been suffering from freezing and thawing-induced damage and deterioration. This paper has analyzed the shallow soil temperatures, the ground temperatures, and the embankment deformations monitored at four sites of the QTH with different route trends and embankment heights in the Southern Tanglha Region (STR) from 2005 to 2015 against the asymmetric damage to the embankments observed in the region. It is concluded that the asymmetrical damage to the embankments of the QTH observed in the STR were controlled by the sunny-shady slope effect (SSSE). Moreover, the following conclusions can be drawn from this study:

(1) The asymmetric damage to embankments has become the main thermal hazard in permafrost regions. Up to 60% of the damage presents distinct asymmetric features, especially in relatively high embankment sections, of which longitudinal cracks and slope collapses are the primary forms.
(2) The SSSE was the leading cause of the induced asymmetric temperature field in the embankments and was characterized by the increase in ground temperature, the descent of the permafrost table, and the expansion of the thawing period in the sunny slopes. The embankment height and the route direction were the primary factors of influence in the SSSE. , the SSSE could be strengthened in the warm permafrost regions to a certain degree.
(3) The asymmetric temperature field in the embankments, resulting from the SSSE, was seen to lead to various degrees of uneven deformation during the operation period. The maximum difference between the deformations of the sunny and shady slopes reached 18 cm and is continuously developing. Some effective measures should be adopted to mitigate or control the SSSE.

Acknowledgments

This work was supported by the National Natural Science Foundation of China (Grant No. 41971095), the Project of Youth Science and Technology New Star in Shaanxi Province of China (2016KJXX-91 and 2019KJXX-93), and the Special Support Plan for High Level Talents in Shaanxi Province of China (Dr. Long Jin).

References

Cheng, G.D., Sun, Z.Z., Niu, F.J., 2008. Application of the roadbed cooling approach in Qinghai-Tibet railway engineering. Cold Reg. Sci. Technol. 53, 241–258.

Chou, Y., Sheng, Y., Chen, J., et al., 2015. Analysis on thermal stability and deformation stability of CMR. Cold Reg. Sci. Technol. 110, 215–222.

Chou, Y., Sheng, Y., Li, Y., et al., 2010. Sunny-shady slope on the thermal and deformation stability of the highway embankment in warm permafrost regions. Cold Reg. Sci. Technol. 63, 78–86.

Chou, Y., Sheng, Y., Wei, Z., et al., 2008. Calculation of temperature differences between the sunny slopes and the shady slopes along the railways in permafrost regions on Qinghai-Tibet Plateau. Cold Reg. Sci. Technol. 53, 346–354.

Gao, S., Wu, Q., Zhang, Z., et al., 2015. Impact of climatic factors on permafrost of the Qinghai-Xizang Plateau in the time-frequency domain. Quat. Int. 374 (2), 174–179.

Jia, H., Zi, F., Yang, G., Li, G., Shen, Y., Sun, Q., Yang, P., 2019. Influence of pore water (ice) content on the strength and deformability of frozen argillaceous siltstone. Rock Mech. Rock Eng. https://doi.org/10.1007/s00603-019-01943-0.

Jin, L., Wang, S., Chen, J., et al., 2012. Study on the height effect of highway embankment in permafrost regions. Cold Reg. Sci. Technol. 83–84, 122–130.

Lai, Y., Ma, W., Zhang, M., et al., 2006. Experimental investigation on influence of boundary conditions on cooling effect and mechanism of crushed-rock layers. Cold Reg. Sci. Technol. 45 (2), 114–121.

Lai, Y., Zhang, S., Zhang, L., et al., 2004. Adjusting temperature distribution under the south and north slopes of embankment in permafrost regions by the ripped-rock revetment. Cold Reg. Sci. Technol. 39 (1), 67–79.

Li, S., Cheng, G., 1996. Map of frozen ground on Qinghai-Xizang Plateau. Gansu Culture Press, Lanzhou.

Liu, H., Niu, F., Niu, Y., 2016. Effect of structures and sunny-shady slopes on thermal characteristics of subgrade along the Harbin-Dalian Passenger. Cold Reg. Sci. Technol. 123, 14–21.

Liu, W., Yu, W., Lu, Y., 2019. Crack damage investigation of paved highway embankment in the Tibtan Plateau permafrost environments. Cold Reg. Sci. Technol. 163, 78–86.

Ming, F., Yu, Q., Li, D., 2018. Investigation of embankment deformation mechanisms in permafrost regions. Transp. Geotech. 16, 21–28.

Ministry of Water Resources of China, 2019. Standard for geotechnical testing method. GB/T 50123-2019. China Planning Press.

Niu, F., Cheng, G., Xia, H., et al., 2006. Field experiment study on effects of duct-ventilated railway embankment on protecting the underlying permafrost. Cold Reg. Sci. Technol. 45 (3), 178–192.

Pei, W., Zhang, M., Li, S., et al., 2018. Laboratory investigation of the efficiency optimization of an inclined two-phase closed thermosyphon in ambient cool energy utilization. Renewable Energy 133, 1178–1187.

Pei, W., Zhang, M., Yan, Z., et al., 2019. Numerical evaluation of the cooling performance of a composite L-shaped two-phase closed thermosyphon (LTPCT) technique in permafrost regions. Sol. Energy 177, 22–31.

Peng, H., Ma, W., Mu, Y., et al., 2015a. Degradation characteristics of permafrost under the effect of climate warming and engineering disturbance along the Qinghai-Tibet Highway. Nat. Hazards. 75, 2589–2605.

Peng, H., Ma, W., Mu, Y., et al., 2015b. Impact of permafrost degradation on embankment deformation of Qinghai-Tibet Highway in permafrost regions. J. Cent. South Univ. 22, 1079–1086.

Sheng, Y., Ma, W., Wen, Z., et al., 2005. Analysis of difference in thermal state between south face slope and north faced slope of railway embankment in permafrost region. Chinese J. Rock Mech. Eng. 24 (17), 3197–3201 (In Chinese).

Shen, Y., Yang, H., Xi, J., et al., 2020. A novel shearing fracture morphology method to assess the influence of freeze–thaw actions on concrete–granite interface. Cold Reg. Sci. Technol. 169 102900.

Song, Y., Jin, L., Zhang, J., 2013. In-situ study on cooling characteristics of two-phase closed thermosyphon embankment of Qinghai-Tibet Highway in permafrost regions. Cold Reg. Sci. Technol. 93, 12–19.

Tai, B., Liu, J., Yue, Z., 2018. Effect of sunny-shady slopes and strike on thermal regime of subgrade along a high-speed railway in cold regions, China. Eng. Geol. 232, 182–191.

Tsytovich, N.A., 1985. The Mechanics of Frozen Ground. Science Press, Beijing (Translated by Zhang Changqing, Zhu Yuanling).

Wang, L., Wang, W., Yu, F., 2015. Thaw consolidation behaviors of embankments in permafrost regions with periodical temperature boundaries. Cold Reg. Sci. Technol. 109, 70–77.

Wang, S., Jin, L., Mu, K., et al., 2019a. The temporal effect of distress developments of frozen embankments in the permafrost regions along the Qinghai-Tibet Highway. J. Test. Eval. 47 (4). https://doi.org/10.1520/JTE20170487.

Wang, T. (Ed.), 2006. Map of the Glaciers, Frozen Ground and Deserts in China. SinoMaps Press, Beijing.

Wang, T., Zhou, G., Wang, J., et al., 2019b. Stochastic coupling analysis of uncertain hidro-thermal properties for embankment in cold regions. Transp. Geotech. 21 100275.

Wu, D., Jin, L., Peng, J., et al., 2014. The thermal budget evaluation of the two-phase closed thermosyphon embankment of the Qinghai-Tibet Highway in permafrost regions. Cold Reg. Sci. Technol. 103, 115–122.

Wu, Q., Hou, Y., Yun, H., et al., 2015. Changes in active-layer thickness and near-surface permafrost between 2002 and 2012 in alpine ecosystems, Qinghai-Xizang (Tibet) Plateau, China. Global Planetary Change 124, 149–155.

Wu, Q., Zhang, T., 2008. Recent permafrost warming on the Qinghai-Tibetan Plateau. J. Geophys. Res. 113, D13108.

Wu, Q., Zhang, T., 2010. Changes in active layer thickness over the Qinghai-Tibetan Plateau from 1995 to 2007. J. Geophys. Res. 115, D09107.

Yu, F., Qi, J., Lai, Y., et al., 2016. Typical embankment settlement/heave patterns of the Qinghai-Tibet highway in permafrost regions: formation and evolution. Eng. Geol. 214, 147–156.

Yu, W., Lai, Y., Zhang, X., et al., 2005. Experimental study on the ventiduct embankment in Permafrost regions of the Qinghai-Tibet Railroad. J. Cold Reg. Eng. 19 (2), 52–60.

Zhang, H., Zhang, J., Wang, E., et al., 2017a. Thermal and settlement analyses under a riverbank over permafrost. Comput. Geotech. 91, 48–57.

Zhang, M., Wang, J., Lai, Y., 2019. Hydro-thermal boundary conditions at different underlying surfaces in a permafrost region of the Qinghai-Tibet Plateau. Sci. Total Environ. 670, 1190–1203.

Zhang, M., Pei, W., Li, S., et al., 2017b. Experimental and numerical analyses of the thermo-mechanical stability of an embankment with shady and sunny slopes in a permafrost region. Appl. Therm. Eng. 127, 1478–1487.

Zhao, L., Wu, Q., Marchenko, S.S., et al., 2010. Thermal state of permafrost and active layer in central Asia during the international polar year. Permafrost Periglac. Process. 21, 198–207.